Numerical Study of Unsteady Free Convective Heat Transfer in Walters-B Viscoelastic Flow over an Inclined Stretching Sheet with Heat Source and Magnetic Field.

Abdulwaheed Jimoh[*]; Moses S. Dada; Amos S. Idowu; and Samson A. Agunbiade

Department of Mathematics, University of Ilorin, Ilorin, Nigeria

E-mail: sesan@unilorin.edu.com[*]
abdulwaheedjimoh@gmail.com
agunbiade1971@gmail.com

ABSTRACT

An investigation was carried out on the numerical study of unsteady free convective heat transfer in Walters-B viscoelastic flow over an inclined stretching sheet with heat source and magnetic field. The dimensionless governing equations are solved using an implicit finite difference method of Crank-Nicolson type. The effects of various parameters on the velocity and temperature fields as well as the coefficient of skin-friction and Nusselt number were presented graphically and in tabulated forms. It is observed that, when the heat source parameter increases, the velocity and temperature increase in the boundary layer.

(Keywords: Crank-Nicolson equation, velocity, temperature, coefficient of skin-friction, Nusselt number, non-Newton fluid flow)

INTRODUCTION

The study of non-Newtonian fluid flow has gained the attention of engineers and scientists in recent times due to its important application in various branches of science, engineering and technology: particularly in chemical and nuclear industries, material processing, geophysics, and bio-engineering. In view of these applications, an extensive range of mathematical models has been developed to simulate the diverse hydrodynamic behavior of these non-Newtonian fluids. In particular, different viscoelastic fluid models like the Rivlin-Ericksen second order model, Oldroyd model, and Johnson-Seagalman model.

The fluids which exhibit the elasticity property of solids and viscous property of liquids are called viscoelastic fluid. These fluid flows are encountered in numerous areas of petrochemical, biomedical and environment engineering including polypropylene coalescence sintering. Consequently, Ahmed et al. (2012), studied magnetic field effect on free convective oscillatory flow between two vertical parallel plates with periodic plate temperature and dissipative heat. Idowu et al. (2013), examined heat and mass transfer of magneto hydrodynamic (MHD) and dissipative fluid flow passing a moving vertical porous plate with variable suction. Alam et al. (2009), presented transient magneto hydrodynamic free convective heat and mass transfer flow with thermophoresis past a radiate inclined permeable plate in the presence of variable chemical reaction and temperature dependent viscosity. Chamkha et al. (2001) investigated the radiation effect on free convection flow past a semi-infinite vertical plate with mass transfer. Devika (2013), further considered the MHD oscillatory flow of a viscoelastic fluid in a porous channel with chemical reaction. Rushi and Sivaraj (2012), obtained MHD Viscoelastic fluid non-Darcy flow along a moving vertical cone. Hady et al (2006), considered the MHD Free convection flow along a vertical wavy surface wiyh heat generation or absorption effect. Hadjinicolaou (1993), studied the heat transfer characteristics in the laminar boundary layer of a viscous fluid over a stretching sheet with viscous dissipation or frictional heating and internal heat generation.

The study of viscos-elastic fluid through porous medial has become the basis of many scientific and engineering applications. This type of flow is of great importance in the petroleum engineering concerned with the movement of oil, gas and water through reservoir of oil or gas field to the hydrologist in the study of the migration of underground water and to the chemical engineering for the purification and filtration processes and in the case like drug permeation through human skin. The principles of this subject are very useful in recovering the water for drinking and irrigation purposes. Many research workers like Alam et al. (2006), examined the free convection heat and mass transfer flow past an inclined semi-infinite heated surface of an electrically conducting and steady viscous incompressible fluid in the presence of a magnetic field and heat generation. Abdus and Mohammed (2006), considered the thermal radiation interaction with unsteady MHD flow past a vertical porous plate immersed in a porous medium. The importance of radiation in the fluid led Muthucumaraswamy and Chandrakala (2006), to study radiative heat and mass transfer effect on moving isothermal vertical plate in the presence of chemical reaction. Muthucumaraswamy and Senthih (2004), investigated the problem Heat and Mass transfer effect on moving vertical plate in the presence of thermal radiation.

In many chemical engineering processes, the chemical reactions do occur between a mass and fluid in which a plate is moving. These processes take place in numerous industrial applications such as polymer production, manufacturing of ceramics or glassware, and food processing. In light of the fact that the combination of heat and mass transfer problems with chemical reaction are of importance in many processes, they have therefore received a considerable amount of attention in recent years. In processes such as drying, evaporation at the surface of a water body, energy transfer in a wet cooling tower and the flow in a desert cooler, heat and mass transfer occur simultaneously. Possible applications of this type of flow can be found in many industries. For example, in the power industry, among the methods of generating electricity is one in which electrical energy is extracted directly from the roving conducting fluid.

Naving Kumar and Sandeep Gupta (2008) also investigated the effect of variable permeability on unsteady two-dimensional free convective flow through a porous bounded by a vertical porous sourface. Sandeep and Sugunamma (2013), studied the effect of inclined magnetic field on unsteady free convective flow of dissipative fluid past a vertical plate. Makinde and Mhone (2005), considered the Heat transfer to MHD oscillatory flow in a channel filled with porous medium. Sharma et al. (2011) have studied the Influence of chemical reaction on unsteady MHD free convective flow and mass transfer through viscous incompressible fluid past a heated vertical plate immersed in porous medium in the presence of heat source. R. Muthucumaraswamy and Ganesan (2001), studied the effect of the chemical reaction and injection on flow characteristics in an unsteady upward motion of an isothermal plate. Mohammed (2009) presented the double-diffusive convection-radiation interaction on unsteady MHD flow over a vertical moving porous plate with heat generation and Soret effects.

Based on these investigations, work has been reported in the field. In particular, the study of heat transfer/heat radiation is of considerable importance in chemical and hydrometallurgical industries. Mass transfer processes include the evaporation of water from a pound to the atmosphere and the diffusion of chemical impurities in lakes, rivers, ocean, or from natural or artificial sources.

Magnetohydrodynamic mixed convection heat transfer flow in porous plate and non-porous media is of considerable interest in the technical field due to its frequent occurrence in industrial technology and geothermal application, high temperature plasma application to nuclear fusion energy conversion, liquid metal fluid and MHD power generation systems combined heat mass transfer in natural convective flows on moving vertical porous plate. Das et al. (2012), studied the MHD Natural Convection Vertical parallel Plates with Oscillatory Wall Temperature. Srinvasa et al. (2010), also studied the finite element analysis of radiation and mass transfer flow past semi-infinite moving vertical plate with viscous dissipation.

Motivated by the above mentioned investigations and applications, in this paper, we analyze the unsteady MHD free convective, thermal radiation, inclined magnetic, and Walters-B' fluid flow over a moving vertical porous plate with variable suction. The results of this parametric study on the flow and heat transfer characteristics are shown graphically and the physical aspects are discussed in detail.

MATHEMATICAL ANALYSES

Consider unsteady two-dimensional hydro magnetic laminar, incompressible, viscous, electrically conducting, and inclined magnetic field past a semi-infinite vertical moving heated porous plate embedded in a porous medium and subjected to a uniform transverse magnetic field in the presence of thermal radiation effect and heat source. According to the coordinate system, the x-axis is taken along the plate in upward direction and y-axis is normal to the plate. The fluid is assumed to be a gray, absorbing-emitting but non-scattering medium. The radiative heat flux in the x-direction is considered negligible in comparison with that in the y-direction [3].

It is assumed that there is no applied voltage of which implies the absence of an electric field. The transversely applied magnetic field and magnetic Reynolds number are very small and hence the induced magnetic field is negligible. Viscous and Darcy resistance terms are taken into account the constant permeability porous medium. The MHD term is derived from an order-of-magnitude analysis of the full Navier-Stokes equation. It is assumed here that the whole size of the porous plate is significantly larger than a characteristic microscopic length scale of the porous medium.

The fluid properties are assumed to be constants except that the influence of density variation with temperature that has been considered in the body-force. Since the plate is semi-infinite in length, therefore all physical quantities are functions of y and t only. Hence, by the usual boundary layer approximations, the governing equations for unsteady flow of a viscous incompressible fluid through a porous medium are:

Continuity Equation

$$\frac{\partial u^*}{\partial y^*}=0 \qquad \textbf{(1)}$$

Linear Momentum Equation

$$\frac{\partial u^*}{\partial t^*}+v^*\frac{\partial u^*}{\partial y^*}=v\frac{\partial^2 u^*}{\partial y^{*2}}-k_0\frac{\partial^3 u^*}{\partial t^* y^{*2}}+g\beta(T^*-T_\infty^*)+\frac{\sigma B_0^2}{\rho}u^*\cos\alpha+\frac{v}{k^*}u^* \qquad \textbf{(2)}$$

Energy Equation

$$\frac{\partial T^*}{\partial t^*}+v^*\frac{\partial T^*}{\partial y^*}=\propto\frac{\partial^2 u^*}{\partial y^{*2}}+\frac{QT}{\rho c_p}(T^*-T_\infty^*)+\frac{v}{c_p}\left(\frac{\partial u^*}{\partial y^*}\right)^2-\frac{1}{\rho c_p}\frac{\partial q_r}{\partial y^*} \qquad \textbf{(3)}$$

The boundary conditions for the velocity, temperature and concentration fields are

$$t^*>0\ ,\ u^*=0\ ,\ T^*\to T_\infty^*\ \text{for as}\ y^*=0$$
$$u^*=0\ ,\ T^*\to T_\infty^*\ \text{as}\ y^*\to\infty \qquad \textbf{(4)}$$

Where y is dimensions coordinates, u^* and v^* are dimensionless velocities, t^* is dimensionless time, T^* is the dimensional temperature, g- the acceleration due to gravity, β - the volumetric coefficient of thermal expansion, β^* is the volumetric coefficient of thermal expansion with concentration, ρ - the density of the fluid, C_p is the specific heat at constant pressure, k^* is the permeability of the porous medium, q_r is the radiation heat flux, B_0- magnetic induction, v- the kinematic viscosity, T_∞^* is wall dimensional temperature respectively, T_∞^*- the free stream temperature far away from the plate, $n^*\theta Re$ is the Reynolds number, k_0 is the dimensional visco-elastic parameter, QT is the dimensional heat generational coefficient, R is the radiation parameter, Pr is Prandtl number, U is velocity, n is the frequency, M is the Hartmann number, K is the permeability parameter, F is Walters-B' viscoelastic, η is the heat source, Gr is thermal Grashot number, $\propto$ is the angle of inclination, and Ec is Eckert number, A is a real positive constant of suction velocity parameter, $<\in$, and $\in A<1$ are small less than unity, i.e., $\in A<<1$, v_0 is a scale of suction velocity normal to the plate.

The constant radiative heat flux term by using the Rosseland approximation is given by:

$$q_w^* = \frac{4\sigma^*}{3k_r^*}\left(\frac{\partial T^{*4}}{\partial y^*}\right)_{y=0} \qquad \textbf{(5)}$$

Where, σ^* is the Stefan-Boltzmann constant and k_r^*- the mean absorption coefficent. It should be noted that by using the Rosseland approximation the present analysis is limited to optically thick fluids. If temperature differences within the flow are sufficient small, then Equation (6) can be linearized by expanding T^{*4} into the Taylor series about T_∞^*, which after neglecting higher order terms takes the form:

$$T^{*4} \cong 4T_\infty^{*3}T^* - 3T^{*4} \qquad \textbf{(6)}$$

$$q_w^* = -\left(\frac{16\sigma T_\infty^*}{3k_r^*}\right) \qquad \textbf{(7)}$$

Substituting Equation (6) and (7), into Equation (3), gives:

$$\frac{\partial T^*}{\partial t^*} + v^*\frac{\partial T^*}{\partial y^*} = \propto \frac{\partial^2 T^*}{\partial y^{*2}} + \frac{1}{\rho c_p}\frac{16\sigma_s}{3k_s}T_\infty^{*3}\frac{\partial^2 T^*}{\partial y^{*2}} + \frac{v}{c_p}\left(\frac{\partial u^*}{\partial y^*}\right)^2 + Q_o(T^* - T) \qquad \textbf{(8)}$$

Introducing the following non-dimensional quantities:

$u = \frac{u^* L (Gr)^{-\frac{1}{2}}}{v}$, $y = \frac{V_0 y^* (Gr)^{\frac{1}{4}}}{vL}$, $t = \frac{vt^*(Gr)^{\frac{1}{2}}}{v^2}$, $\theta = \frac{T^* - T_\infty^*}{T_W^* - T_\infty^*}$, Pr$= \frac{v\rho C_p}{k} = \frac{v}{\alpha}$,

Sc = $\frac{v}{D}$, Gr = $g\beta v\frac{(T_W - T_\infty)L^3}{v^2}$, Ec = $\frac{v^2 G_r}{L^2 C_p (T_W - T_\infty)}$,R=$\frac{4\sigma_s T_\infty'^3}{k_s k}$, M=$\frac{\sigma B_0^2 L^2}{\rho (G_r)^{\frac{1}{2}}}$,

$$\eta T = \frac{QTL^2}{\mu C_p (G_r T)^{\frac{1}{2}}}, \quad F = \frac{k_0}{L^2}(G_r T)^{\frac{1}{2}} \qquad \textbf{(9)}$$

Into the Equations (2) and (8) with Equation (1) identically satisfied the following set of differential equations:

$$\frac{\partial u}{\partial t} - (1 + \in Ae^{nt})\frac{\partial u}{\partial y} = \frac{\partial^2 u}{\partial y^2} + G_r\theta - F\frac{\partial^3 u}{\partial t \partial y^2} - \left(M\cos\alpha + \frac{1}{k}\right)u \qquad \textbf{(10)}$$

$$\frac{\partial \theta}{\partial t} - (1 + \in Ae^{nt})\frac{\partial \theta}{\partial y} = \frac{1}{P_r}\left(1 + \frac{4R}{3}\right)\frac{\partial^2 \theta}{\partial y^2} + \eta T\theta + \text{Ec}\left(\frac{\partial u}{\partial y}\right)^2 \qquad \textbf{(11)}$$

The boundary conditions (4) are given by the following dimensionless form:

$$t^* > 0,\ u^* = 0,\ \theta^* \to \theta_\infty^* \text{ as } y^* = 0$$

$$u^* = 0,\ \theta^* \to \theta_\infty^* \text{ as } y^* \to \infty \qquad \textbf{(12)}$$

The dimensionless local value of skin friction τ and Nusselt number Nu can be characterized in order by

$$\tau = -\left(\frac{\partial u}{\partial y}\right)_{y=0} \qquad \textbf{(13)}$$

$$\text{Nu} = -\left(\frac{X\left(\frac{\partial\theta}{\partial y}\right)_{y=0}}{\theta}\right)_{y=0} \tag{14}$$

The average of skin friction, average of Nusselt number (Nu) in dimensionless form can be written as:

$$\tau = -\int_0^1 \left(\frac{\partial u}{\partial y}\right)_{y=0} \mathrm{dX} \tag{15}$$

$$\text{Nu} = -\int_0^1 \left(\frac{X\left(\frac{\partial\theta}{\partial y}\right)_{y=0}}{\theta}\right)_{y=0} dX \tag{16}$$

METHOD OF SOLUTION

In order to solve the non-linear coupled Equation (10) and (16) under the initial and boundary condition (19), an implicit finite difference scheme of crank-Nicolson type has been employed. The finite difference equations corresponding to Equations (10) and (16) are discretized using the Crank-Nicolson Method as follows:

$$\frac{U_{i,j}^{n+1}-U_{i,j}^{n}}{\Delta t} - (1+\in Ae^{nt})\frac{\left(U_{i,j+1}^{n+1}-U_{i,j-1}^{n+1}+U_{i,j+1}^{n}-U_{i,j-1}^{n}\right)}{4\Delta t} =$$

$$\left(1+\frac{F}{\Delta t}\right)\frac{\left(U_{i,j-1}^{n+1}-2U_{i,j}^{n}+U_{i,j+1}^{n+1}-U_{i,j-1}^{n}-2U_{i,j}^{n}+U_{i,j+1}^{n}\right)}{2(\Delta y)^2} + G_r\left(\frac{\theta_{i,j}^{n+1}-\theta_{i,j}^{n}}{2}\right) - \left(M\cos\propto+\frac{1}{k}\right)\left(U_{i,j}^{n+1}-U_{i,j}^{n}\right) \tag{17}$$

$$\frac{\theta_{i,j}^{n+1}-\theta_{i,j}^{n}}{\Delta t} - (1+\in Ae^{nt})\frac{\left(\theta_{i,j+1}^{n+1}-\theta_{i,j-1}^{n+1}+\theta_{i,j+1}^{n}-\theta_{i,j-1}^{n}\right)}{4\Delta t} =$$

$$\frac{1}{Pr}\left(1+\frac{4R}{3}\right)\frac{\left(\theta_{i,j-1}^{n+1}-2\theta_{i,j}^{n}+\theta_{i,j+1}^{n+1}-\theta_{i,j-1}^{n}-2\theta_{i,j}^{n}+\theta_{i,j+1}^{n}\right)}{2(\Delta y)^2} + \text{Ec}\frac{\left(U_{i,j+1}^{n}-U_{i,j-1}^{n}\right)^2}{2\Delta y} + \eta T\left(\theta_{i,j}^{n+1}-\theta_{i,j}^{n}\right) \tag{18}$$

$t^* \leq 0$, $u^* = 0$, $\theta = 0$ for all y

$t^* > 0$, $= 0$, $\theta = 1$ for $y = 0$

$u = 0$, $\theta = 0$ as $y = \infty$ **(19)**

Where Δ is a dimensionless time-step, and Δy is a dimensionless finite difference grid size in the y-direction, i designate the grid point along the x-direction, j along the $y -$ direction and n in the time variable t. Here the region of integration is considered as a rectangle with max $y_{max} = 26$ where y_{max} corresponds to y_∞ which lies well outside the momentum thermal layer, after some preliminary numerical experiments such that the boundary conditions of (19) are satisfied within the tolerance limit 10^{-5}. The mesh sizes have been fixed as $\Delta y = 0.16$ with time step $\Delta t = 0.01$.

The values of the velocity (u) and temperature (θ) at two consecutive time steps are less than 10^{-5} at all grid points. The scheme is unconditionally stable. The local truncation error is $0(\Delta t^2 + \delta y^2)$ and it tends to zero as Δt and Δy tend to zero. It follows that the Crank-Nicolson Method is compatible. Stability and compatibility ensure the convergence.

RESULTS AND DISCUSSIONS

Numerical evaluation for the solutions of this problem is performed and the results are illustrated graphically in Figures 1 – 13 for the interesting features of significant parameters on velocity, temperature local skin friction and local Nusselt number. Throughout the computations we employ A=0.5, t=1.0, n=0.1 and ϵ =0.001, while R, kr^2 , Sc, Gr, M, Pr, η , and k are varied in order to account for their effects.

Figure 3 shows the effect of radiation R on velocity. It is observed that as the value of R increases, the velocity increases with an increasing in the flow boundary layer thickness. Thus, thermal radiation enhances the flow. The effect of radiation parameter R on the temperature profiles are presented in Figure 10. It shows that, as the value of R increases the temperature profiles increases, with an increasing in the thermal boundary layer thickness.

The velocity profiles for different values of Grashof number (Gr) are described in Figure 1. It is observed that an increasing in Gr leads to a rise in the values of velocity and temperature. Here the Grashof number represents the effect of the free convection currents. Physically, Gr>0 means heating of fluid of cooling of the boundary surface, Gr<0 means cooling of the fluid of heating of the boundary surface and Gr=0 corresponds to the absence of free convection current. In addition, the curves show that the peak value of velocity increases rapidly near the wall of the porous plate as Grashof number increases, and then decays to the relevant free stream velocity. Figure 9 shows that, as the value of Gr increase the temperature profiles decreases

Figure 2 and Figure 15 show that the effect of increasing values of M parameter results in decreasing velocity distribution while increase in temperature across the boundary layer because of the application of transfer magnetic field will result a restrictive type force(Lorenz force) similar to drag force which tends to resist the fluid and this reducing its velocity.

The velocity profiles across the boundary layer for different values of Prandtl number (Pr) are plotted in Figure 4 and Figure 11. The results shows that the effect of increasing values of Pr results in a decreasing the velocity and temperature, while it peak up again at the value of 1.7 and 7.

It is observed from Figure 17 that an increase in inclined angle ψ results in a decreasing the thermal boundary layer thickness and more uniform temperature distribution across the boundary layer. Figure 18 shows that the effect of inclined angle on the velocity profile. It shows that an increase in the inclined angle parameter increase the velocity profile.

It is observed from Figure 6 that as velocity profiles for different values of the permeability (K). Clearly, as K increases the peak value of velocity tends to increase. These results could be very useful in deciding the applicability of enhanced oil recovery in reservoir engineering. Also, Figure 16 shows the increasing in permeability (K) while the temperature decreases.

Figure 5 and Figure 12 shows the effects of Eckert number on velocity and temperature, as Eckert number increases the velocity increases and temperature distribution across the boundary layer decreases.

It is observed from Figure 7 that an increase in visco-elastic parameter F results in a decreasing the thermal boundary layer thickness and more uniform temperature distribution across the boundary layer. Figure 13 shows that the effect of visco-elastic parameter on the velocity profile. It shows that an increasing the Walters-B' visco-elastic parameter increase the velocity profile.

Figure 8 and Figure 14 shows that the effect of increasing values of η parameter results in an increasing velocity distribution while increase in temperature across the boundary layer.

Table 1: Effect of R on velocity ,$n = 0.1$, $t = A = M = 1$, $\epsilon = 0.01$, $Pr = 0.71$, $Ec = 0.001$, $Gr = 2$, $k = 1.5$, $\alpha = \pi/2$, $\eta = 0$ and $F = 0.0$.

R	C_f
0	0.4012
1	0.5122
3	0.5578
4	0.5637

Table 2: Effect of Ec on velocity ,$n = 0.1$, $t = A = M = R = 1$, $\epsilon = 0.01$, $Pr = 0.71$, $Gr = 2$, $k = 1.5$, $\alpha = \pi/2$, $\eta = 0$ and $F = 0.0$.

Ec	C_f
3	0.5172
6	0.5224
9	0.5278
12	0.5334

Table 3: Effect of Gr on velocity ,$n = 0.1$, $t = A = M = R = 1$, $\epsilon = 0.01$, $Pr = 0.71$, $Ec = 0.001$, $k = 1.5$, $\alpha = \pi/2$, $\eta = 0$ and $F = 0.0$.

Gr	C_f
2	1.0243
4	2.0487
6	3.0733
8	4.0981

Table 4: Effect of$M$ on velocity ,$n = 0.1$, $t = A = R = 1$, $\epsilon = 0.01$, $Pr = 0.71$, $Ec = 0.001$, $Gr = 2$, $k = 1.5$, $\alpha = \pi/2$, $\eta = 0$ and $F = 0.0$.

M	C_f
2	0.4429
4	0.3542
6	0.3022
8	0.2675

Table 5: Effect of Pr on velocity ,$n = 0.1$, $t = A = M = R = 1$, $\epsilon = 0.01$, $Ec = 0.001$, $Gr = 2$, $k = 1.5$, $\alpha = \pi/2$, $\eta = 0$ and $F = 0.0$.

Pr	C_f
o.60	0.5267
0.71	0.5122
1.7	0.3970
7.0	0.1531

Table 6: Effect of k on velocity ,$n = 0.1$, $t = A = M = R = 1$, $\epsilon = 0.01$, $Pr = 0.71$, $Ec = 0.001$, $Gr = 2$, $\alpha = \pi/2$, $\eta = 0$ and $F = 0.0$.

k	C_f
1.5	1.6765
2.0	2.0768
2.5	2.3327
3.0	2.5088

Table 7: Effect of α on velocity ,$n = 0.1$, $t = A = M = R = 1$, $\epsilon = 0.01$, $Pr = 0.71$, $Ec = 0.001$, $Gr = 2$, $k = 1.5$, $\eta = 2$ and $F = 0.0001$.

α	C_f
$\pi/2$	1.6382
$\pi/4$	1.3214
$\pi/6$	1.2678
$\pi/8$	1.2496

Table 8: Effect of η on velocity ,$n = 0.1$, $t = A = M = 1, R = 2$, $\epsilon = 0.01$, $Pr = 0.71$, $Ec = 4$, $Gr = 2$, $k = 1.5$, $\alpha = \pi/2$ and $F = 0.0002$.

η	C_f
1	0.8149
3	0.8184
5	0.8217
7	0.8249

Table 9: Effect of F on velocity ,$n = 0.1$, $t = A = M = R = 1$, $\epsilon = 0.01$, $Pr = 0.71$, $Ec = 1$, $Gr = 2$, $k = 1.5$, $\alpha = \pi/2$ and $\eta = 0$.

F	C_f
0.0001	0.6033
0.0002	0.7356
0.0003	0.9540
0.0004	1.3424

Table 10: Effect of Gr on Temperature , $n = 0.1$, $t = A = M = R = 1$, $\epsilon = 0.01$, $Pr = 0.71$, $Ec = 0.001$, $k = 1.5$, $\alpha = \pi/2$, $\eta = 0$ and $F = 0.0$.

Gr	C_f
2	3.8525
4	3.8522
6	3.8517
8	3.8509

Table 11: Effect of k on Temperature , $n = 0.1$, $t = A = M = 1, R = 2$, $\epsilon = 0.01$, $Pr = 0.71$, $Ec = 4$, $Gr = 2$, $\alpha = \pi/2$, $\eta = 7$ and $F = 0.0004$.

k	C_f
1.5	3.0659
2.0	2.4857
2.5	2.0516
3.0	1.7248

Table 12: Effect of α on Temperature , $n = 0.1$, $t = A = M = R = 1$, $\epsilon = 0.01$, $Pr = 0.71$, $Ec = 0.001$, $Gr = 2$, $k = 1.5$, $\eta = 2$ and $F = 0.0001$.

α	C_f
$\pi/2$	3.2547
$\pi/4$	3.5013
$\pi/6$	3.5372
$\pi/8$	3.5490

Table 13: Effect of Pr on Temperature , $n = 0.1$, $t = A = M = R = 1$, $\epsilon = 0.01$, $Ec = 0.001$, $Gr = 2$, $k = 1.5$, $\alpha = \pi/2$, $\eta = 0$ and $F = 0.0$.

Pr	C_f
0.60	3.8923
0.71	3.8526
1.7	4.0402
7.0	37.5066

Table 14: Effect of M on Temperature , $n = 0.1$, $t = A = R = 1$, $\epsilon = 0.01$, $Pr = 0.71$, $Ec = 0.001$, $Gr = 2$, $k = 1.5$, $\alpha = \pi/2$, $\eta = 0$ and $F = 0.0$.

M	C_f
2	3.9258
4	3.9339
6	3.9374
8	3.9393

Table 15: Effect of Ec on Temperature , $n = 0.1$, $t = A = M = R = 1$, $\epsilon = 0.01$, $Pr = 0.71$, $Gr = 2$, $k = 1.5$, $\alpha = \pi/2$, $\eta = 0$ and $F = 0.0$.

Ec	C_f
3	3.7729
6	3.6898
9	3.6031
12	3.5334

Table 16: Effect of R on Temperature , $n = 0.1$, $t = A = M = 1$, $\epsilon = 0.01$, $Pr = 0.71$, $Ec = 0.001$, $Gr = 2$, $k = 1.5$, $\alpha = \pi/2$, $\eta = 0$ and $F = 0.0$.

R	C_f
0	4.0202
1	3.8526
3	4.0878
4	4.1649

Table 17: Effect of F on Temperature , $n = 0.1$, $t = A = M = R = 1$, $\epsilon = 0.01$, $Pr = 0.71$, $Ec = 0.001$, $Gr = 2$, $k = 1.5$, $\alpha = \pi/2$ and $\eta = 0$.

F	C_f
0.0001	3.9043
0.0002	3..8799
0.0003	3.8272
0.0004	3.6963

Table 18: Effect of η on Temperature , $n = 0.1$, $t = A = M = R = 1$, $\epsilon = 0.01$, $Pr = 0.71$, $Ec = 0.001$, $Gr = 2$, $k = 1.5$, $\alpha = \pi/2$ and $F = 0.0$.

η	C_f
1	3.7890
3	3.8203
5	3.8530
7	3.8871

Tables (1)-(9) for Velocity: The effects of the heat source /sink parameter and Walters-B' visco-elastic on the skin- friction coefficient. It is observed from this table that as heat source or sink parameter increases, the skin-friction coefficients increases, as either the Porosity Permeability or inclined angle Parameter effect increases, skin-friction coefficient decreases. Also decreases in the Prandtl number Parameter and Magnetic field Parameter effect, the skin-friction coefficient increases

Tables (10)-(18) for Temperature: As the heat source /sink η, inclined angle α, magnetic M, radiation R, parameter increase the Nusselt number increases, Walters-B' visco-elastic F, Grashof number for heat transfer, Permeability parameter, Prandtl number, Eckert number, the Nusselt number also decrease. Also decrease in the magnetic field Parameter effect, the skin-friction coefficient increase.

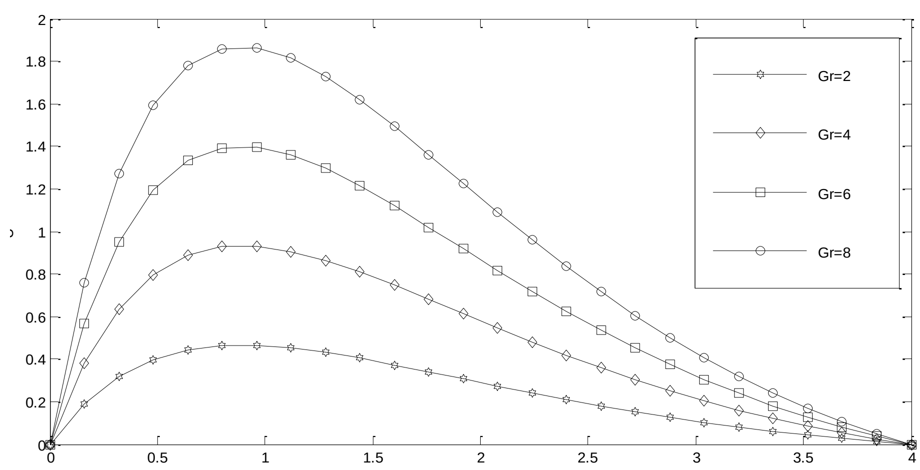

FIG.1.Velocity Profiles for different values of Gr

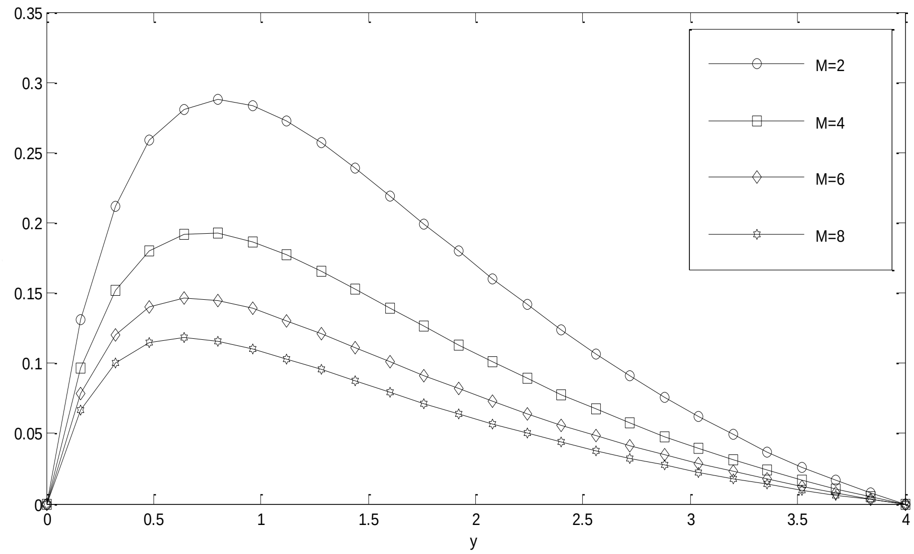

FIG. 2.Velocity Profiles for different values of M

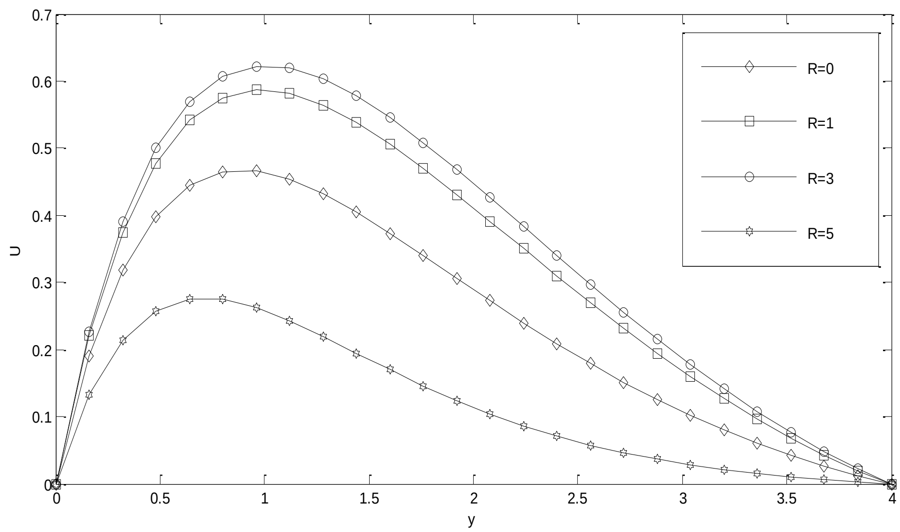

FIG.3.Velocity Profiles for different values of R

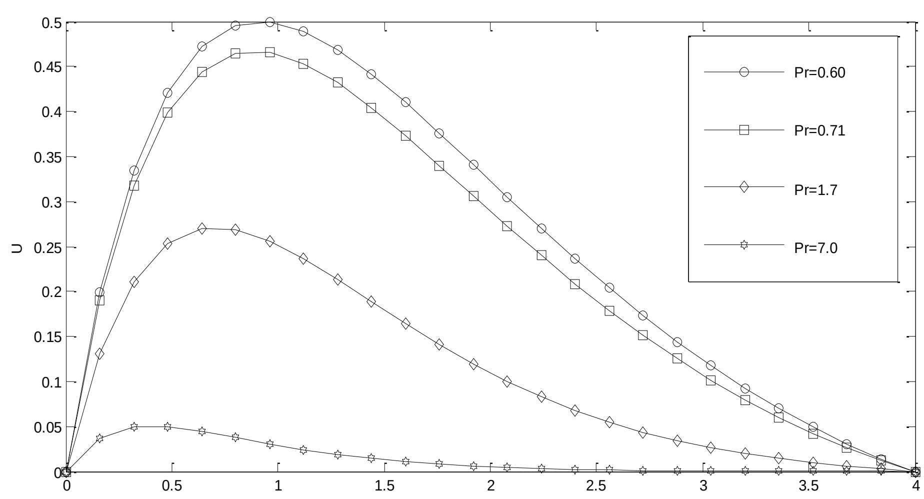

FIG.4.Velocity Profiles for different values of Pr

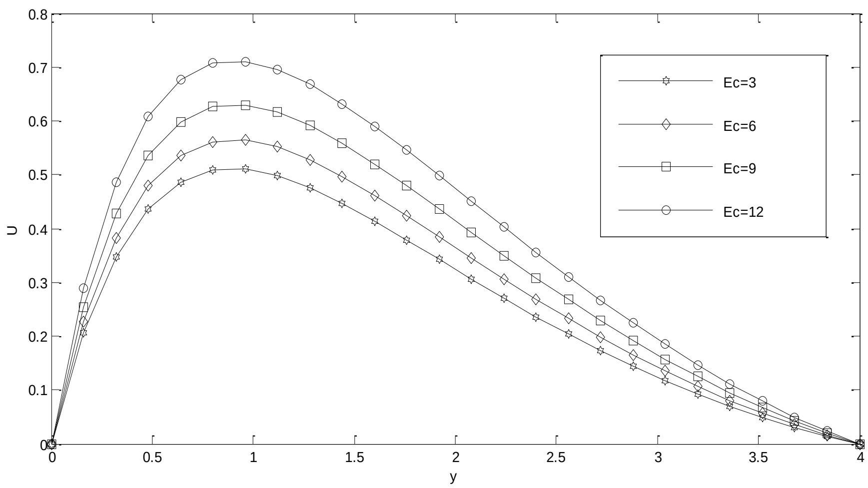

FIG 5. Velocity Profiles for different values of Ec

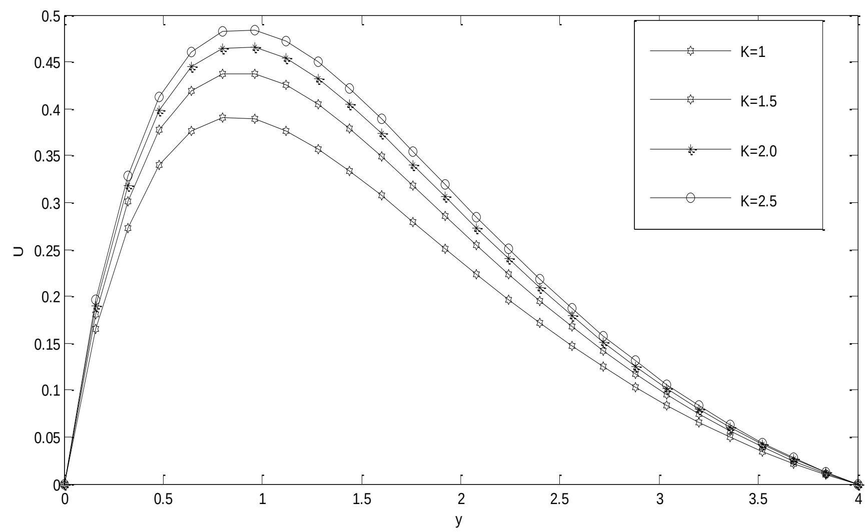

FIG 6. Velocity Profiles for different values of K

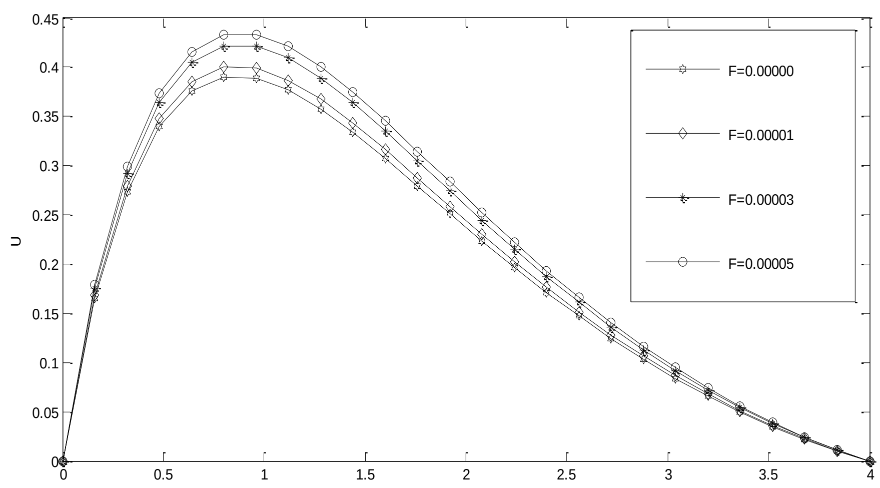

FIG 7. Velocity Profiles for different values of F

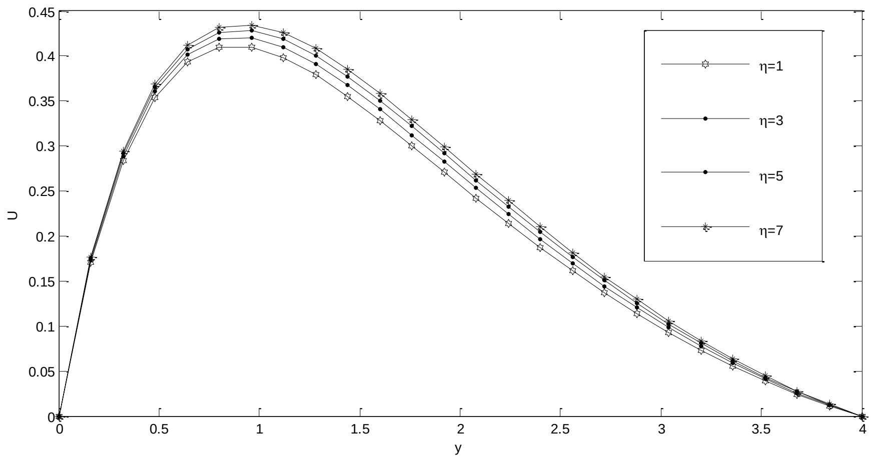

FIG 8. Velocity Profiles for different valus of η

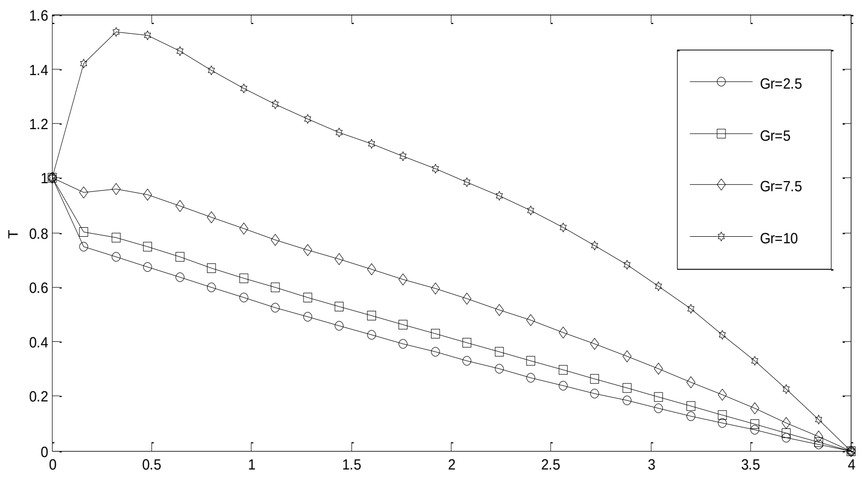

FIG 9. Temperature Profiles for different values of Gr

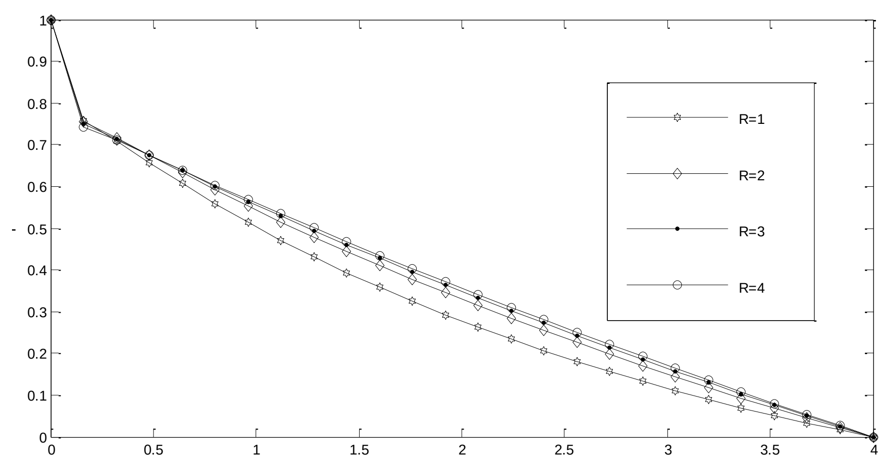

FIG 10.Temperature Profiles for various values of R

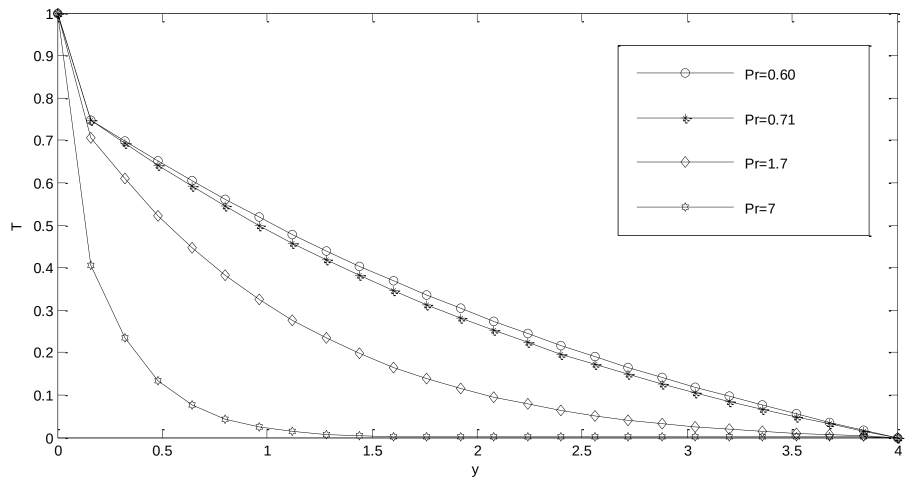

FIG 11. Temperature Profiles for different values of Pr

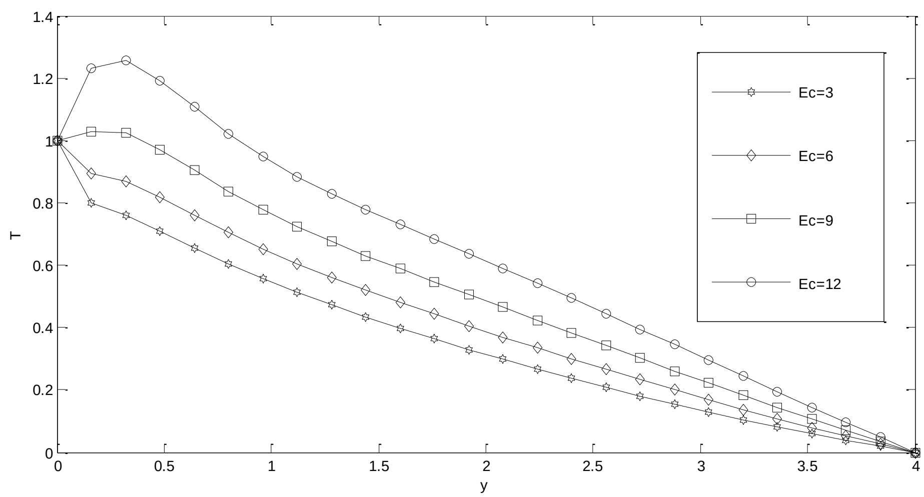

FIG. 12. Temperature Profiles for different values of Ec

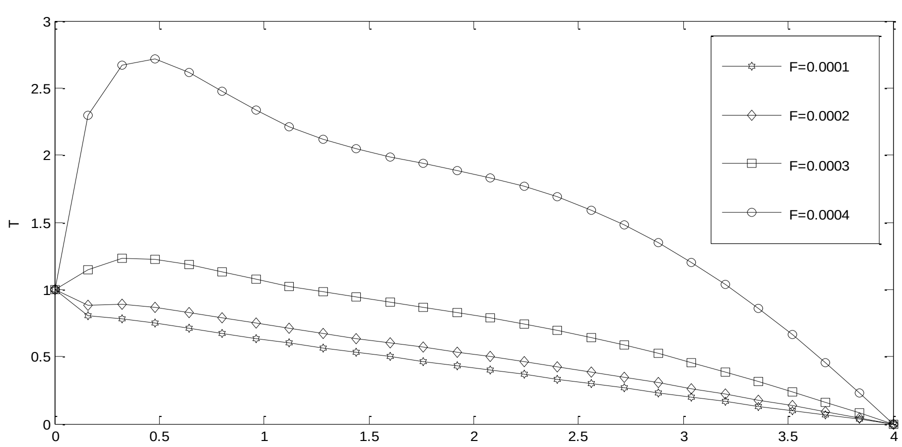

FIG. 13. Temperature Profiles for different values of F

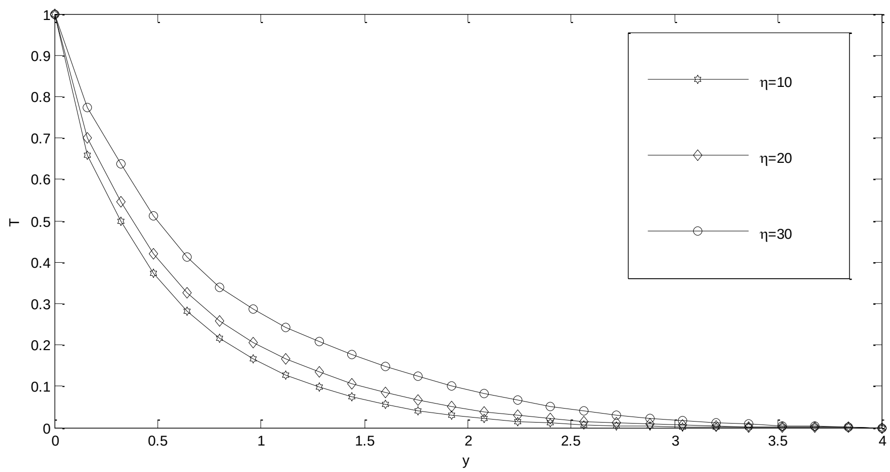

FIG.14.Temperature Profiles for different values of η

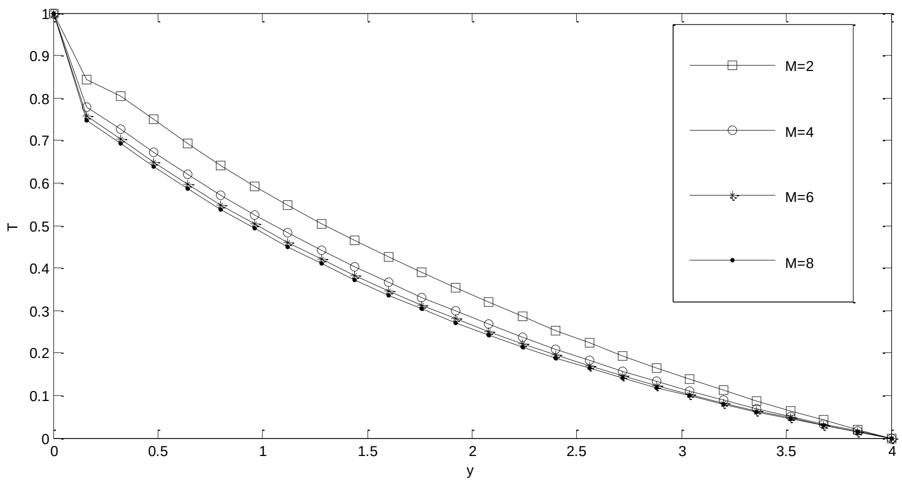

FIG. 15.Temperature Profiles for different values of M

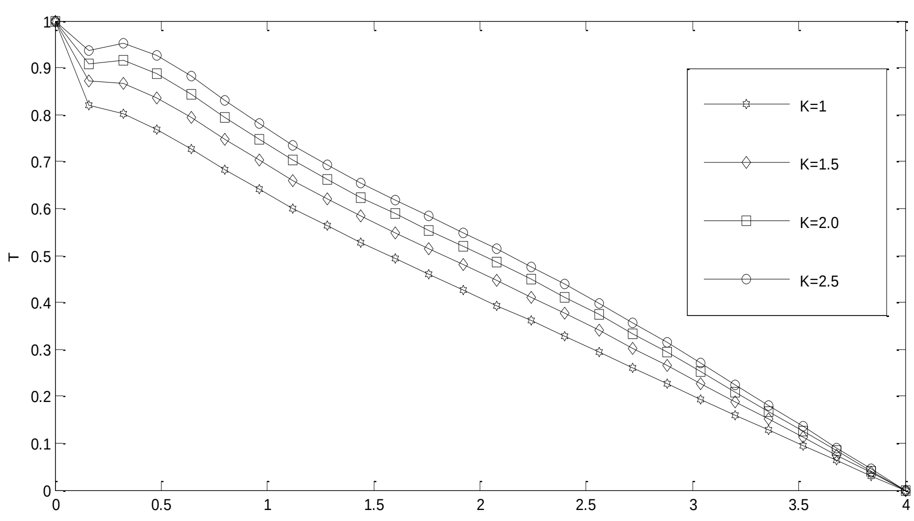

FIG.16.Temperature Profiles for different values of K

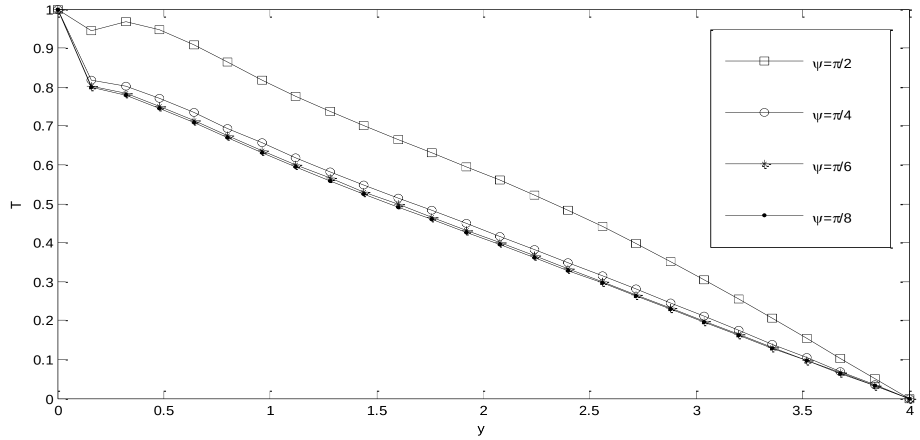

FIG.17.Temperature Profiles for different values of ψ

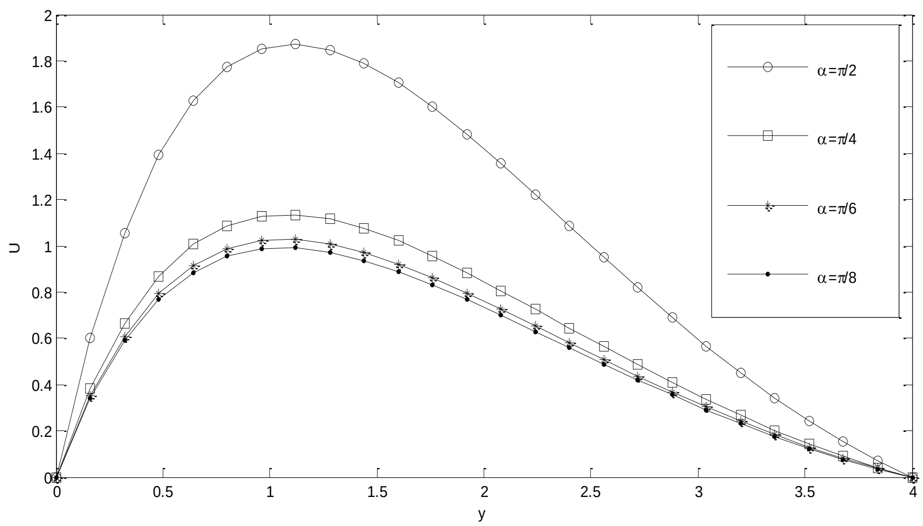

FIG.18.Velocity Profiles for different values of α

CONCLUSION

From the present study, it can be concluded that:

1. The effect of suction parameter is dominating on the velocity and temperature profiles. So, using suction boundary layer growth can be stabilized.

2. The buoyancy parameter has a significant effect.

3. Using magnetic field, we can control the heat transfer flow characteristics.

4. The effect of heat source parameter is very worthy.

5. A rise in the velocity leads to a fall in size of the temperature at the Grashof number (Gr).

6. As velocity and temperature increases the Porosity Parameter (K) also amplify while it falls in temperature.

7. The velocity increases with an increase in the Prandtl number (Pr).

8. A rise in the inclined angle parameter (α) leads to the acceleration of the temperature while the velocity decreases.

9. The size of fluid velocity amplify with the increase of Eckert number (Ec), while the temperature reduces as Eckert number increases.

10. The level of fluid temperature rise while the velocity fall with the rise of Magnetic Parameter (M).

11. The velocity as well as temperature increases with an increase in radiation.

12. The size of fluid velocity amplify with the increase of Walters-B' visco-elastic (F), while the temperature reduces as the value of Walters-B' visco-elastic flow (F), increase.

REFERENCES

1. Abdus Samad, M.D. and M.R. Mohammed. 2006. "Thermal Radiation Interaction with Unsteady MHD Flow Past a Vertical Porous Plate Immersed in a Porous Medium".

2. Ahmed, N., K. Sarma, and D.P. Baruna. 2012. "Magnetic Field Effect on Free Convective Oscillatory Flow between Two Vertical Parallel Plates with Periodic Plate Temperature and Dissipative Heat". *Applied Mathematical Sciences*. 6(39):1913-1924.

3. Alam, M.S., M.M. Rahman, and M.A. Sattar. 2006. "MHD Free Convective Heat and Mass Transfer Flow Past an Inclined Semi-Infinite Heated Surface of an Electrically Conducting and Steady Viscous Incompressible Fluid in the Presence of a Magnetic Field and Generation Thamasat". *Int. J.Sci.Tech*. 11(4):1-8.

4. Alam, M.S., M.M. Rahman, and M.A. Sattar. 2009. "Transient Magneto Hydrodynamic Free Convective Heat and Mass Transfer Flow with Thermophoresis Past a Radiate Inclined Permeable Plate in the Presence of Variable Chemical Reaction and Temperature Dependent Viscosity". *Nonlinear Analysis: Modeling and control.* (14):3-20.

5. Chamkha, A.J., H.S. Takhar, and V.M. Soundalgekar . 2001. "Radiation Effect on Free Convection Flow Past a Semi-Infinite Vertical Plate with Mass Transfer". *Chem. Engr. J*. 84:335-342.

6. Devika, B., P.V. Satya Narayana, and S. Venkataramana. 2013. "MHD Oscillatory Flow of a Viscoelastic Fluid in a Porous Channel with Chemical Reaction". *International Journal of Engineering and Science Invention*. ISSN (online): 2319-6734, ISSN(print):2319-6726.

7. Das, S., B.C. Sarkar, and R.N. Jana . 2012. "MHD Natural Convection Vertical Parallel Plates with Oscillatory Wall Temperature". *J. Comp. and Math. Sci.* 3(4):426-438.

8. Gnaneshwara, R.M. and R.N. Bhaskar. 2009. "Radiation and Mass Transfer Effect on an Unsteady MHD Free Convection Flow Past a Heated Vertical Porous Plate with Viscous Dissipation". *Int. J. of Appl. Math and Mech*. 6(6):96-110.

9. Hady, F.M., R.A. Mohammed, and A. Mahdy. 2006. "MHD Free Convection Flow along a Vertical Wavy Surface with Heat Generation or Absorption Effect". *Int. Comm Heat Mass Transfer.* 33:1253-1263.

10. Hossain, M.A., M.M. Molla, and L.S. Yaa. 2004. "Natural Convection Flow along a Vertical Wavy Surface Temperature in the Presence of Heat Generation/Absorption". *Int. J. Thermal Science*. 43:157-163.

11. Idowu, A.S., M.S. Dada, and A. Jimoh. 2013. "Heat and Mass Transfer of Magneto Hydrodynamic (MHD) and Dissipative Fluid Flow Pass a Moving Vertical Porous Plate with Variable Suction". *Mathematical Theory and Modeling*. ISSN: 2224-5804(Paper), ISSN:2225-0522(online). 3(3).

12. Kim, Y.J. and A.G. Fedorov. 2003. "Transient Mixed Radiation Convection Flow of a Micro Polar Fluid Past a Moving, Semi-Infinite Vertical Porous Plate". *International Journal of Heat and Mass Transfer*. 46:1751-1758.

13. Makinde, D.O. and P.Y. Mhone. 2005. "Heat Transfer to MHD Oscillatory Flow in a Channel Filled with Porous Medium". *Room. J. Phys*. 50:931-938.

14. Mohamed, R.A. 2009. "Double-Diffusive Convection-Radiation Interaction on Unsteady MHD Flow over a Vertical Moving Porous Plate with Heat Generation and Soret Effects". *Applied Mathematics Science*. 3(13):629-651.

15. Muthucumaraswamy, R. and P. Chandrakala. 2006. "Radiative Heat and Mass Transfer Effect on Moving Isothermal Vertical Plate in the Presence of Chemical Reaction". *International Journal of Applied Mechanics and Engineering*. 11:639-646.

16. Muthucumaraswamy, R. and K.G. Senthih. 2004. "Heat and Mass Transfer Effects on Moving Vertical Plate in the Presence of Thermal Radiation". *Theoretical Applied Mechanics*. 31:35-46.

17. Muthucumaraswamy, R. and Ganesan, P.:Effect of the chemical reaction and injection on flow characteristics in an unsteady motion of an isothermal plate, J.Appl. Mech. Tech.Phys. (2001), 42, 65-667.

18. Naving, K. and G. Sandeep. 2008. "Effect of Variable Permeability on Unsteady Two-Dimensional Free Convective Flow through a

Porous Bounded by a Vertical Porous Surface". *Asian J. Exp. Sci*. 22(3):275-284.

19. Rushi, K.B. and R. Sivaraj. 2012. "MHD Viscoelastic Fluid Non-Darcy Flow along a Moving Vertical Cone". *Int. J. of Appl. Math. and Mech*. . 8(11):69-81.

20. Sandeep, N. and V. Sugunamma. 2013. "Effect of Inclined Magnetic Field on Unsteady Free Convective Flow of Dissipative Fluid past a Vertical Plate. 1(1):6-23. ISSN: 2336-0062.

21. Sharma, P.R., K. Navin, and S. Pooja. 2011. "Influence of Chemical Reaction and Radiation on Unsteady MHD Free Convective Flow and Mass Transfer through Viscous Incompressible Fluid Past a Heated Vertical Plate Immersed in Porous Medium in the Presence of Heat Source".

22. Sugunamma and Sandeep. 2011. "Unsteady Hydromagnetic Free Convective Flow of a Flux". Int. J. of Mathematics and Computer Research". 1(1):37-50.

23. Srinivasa, R.V. and L. Anand Babu. 2010. "Studied the Finite Element Analysis of Radiation and Mass Transfer Flow Past Semi-Infinite Moving Vertical Plate with Viscous Dissipation". *ARPN Journal of Engineering and Applied Sciences*. 5(11).

24. Vajravelu, K. and A. Hdjinicolaou. 1993. "Heat Transfer in a Viscous Fluid Over a Stretching Sheet with Viscous Dissipation and Internal Heat Generation". *Int. Comm. Heat Mass Transfer*. 20:417-430.

SUGGESTED CITATION

Jimoh, A., M.S. Dada, A.S. Idowu, and S.A. Agunbiade. 2015. "Numerical Study of Unsteady Free Convective Heat Transfer in Walters-B Viscoelastic Flow over an Inclined Stretching Sheet with Heat Source and Magnetic Field". *Pacific Journal of Science and Technology*. 16(1):60-76.

Pacific Journal of Science and Technology